3-D numerical simulation of structurally controlled, progressive failure of a large-diameter experiment borehole

Chenxi Zhao[1*^], Qinghua Lei[1], Martin Ziegler[2] and Simon Loew[1]

[1] Chair of Engineering Geology, Department of Earth Sciences, ETH Zurich, Zurich, Switzerland
[2] Federal Office of Topography swisstopo. Zurich, Switzerland

* Corresponding author information: chenzhao@ethz.ch, +41 779 665 681
^ Presenting author

1. Background

Underground excavation often causes progressive damage evolution and fracture propagation in rocks leading to over-breaks around excavations (Martin et al. 2003; Martin & Christiansson 2009; Martino & Chandler 2004; Read 2004). This overbreak phenomenon tends to be strongly affected by faults and fractures that impose essential structural controls on the failure and instability pattern. To gain a better understanding of the influence by pre-existing geological structures on excavation-induced damage evolution, we developed a high-fidelity 3-D geomechanics model to simulate the progressive failure experiment at the Mont Terri Underground Laboratory (MT URL), Switzerland. Our research aims at exploring the short-term (during the borehole drilling) and long-term (over years after the borehole completion) spatio-temporal evolution of fracture displacement and crack growth around a large experiment borehole in Opalinus Clay shale, and investigating the physical mechanisms that drive the structurally controlled overbreak phenomenon around the borehole. Deep damage and overbreaks are not only critical for short-term stability of an excavation in Opalinus Clay shale but could substantially reduce the effective thickness of the geological barrier in a nuclear waste repository of a long-term service period. Structurally controlled failure may initiate immediately during excavation and subsequent damage of the geological barrier could further develop in a progressive manner, i.e., during decades to thousands of years, driven by hydromechanically and thermomechanically coupled processes and delayed deterioration of support structures. Thus, it is of central importance to evaluate fault zone hazard scenarios related to repository construction and long-term safety (Ziegler and Loew 2020).

2. Progressive failure (PF) project

The PF experiment is conducted in the MT URL at Niche MI to investigate the spatio-temporal evolution of structurally controlled overbreaks during underground excavation. At the end of 2020, an experimental borehole with a diameter of 0.6 m and length of 12.9 m that intersects a major fault zone and fractured hanging wall as well as foot wall rock masses was drilled and the subsequent progressive failure around the borehole has been systematically monitored using electrical resistivity and seismic tomography, as well as camera-based imaging. Visible damage of the experimental borehole includes (i) stress-induced borehole wall breakouts that formed rapidly during drilling and increased in size over time, (ii) irreversible slip along a prominent, gently dipping fault plane in the hanging wall of the major fault zone and associated new fracture growth. To investigate the damage pattern, evolution, and extent, we built a 3DEC model of the fractured rock mass volume and simulated the borehole excavation process. Ziegler et al. (this volume) present the in-situ experiment setup and relevant observational datasets.

3. Model approach and setup

Figure 1 presents the workflow of the model setup and simulation procedures. Firstly, to represent pre-existing discontinuities, a realistic discrete fracture network including a large fault zone and mesoscale fractures was constructed based on borehole logs. Then, a multiscale model involving inner and outer subdomains was built. The size of the entire domain is 15 m × 15 m × 15 m, with an inner region of 15 m × 4.2 m in the model's center. The inner domain is subdivided into numerous blocks by the discontinuities with each block further discretized into Voronoi cells that allow new fractures to propagate. The outer region is treated as a continuum associated with equivalent properties (Thoeny 2014; Table 1) while the major fault zone is explicitly represented across the entire model domain (Figure 1, middle panel).

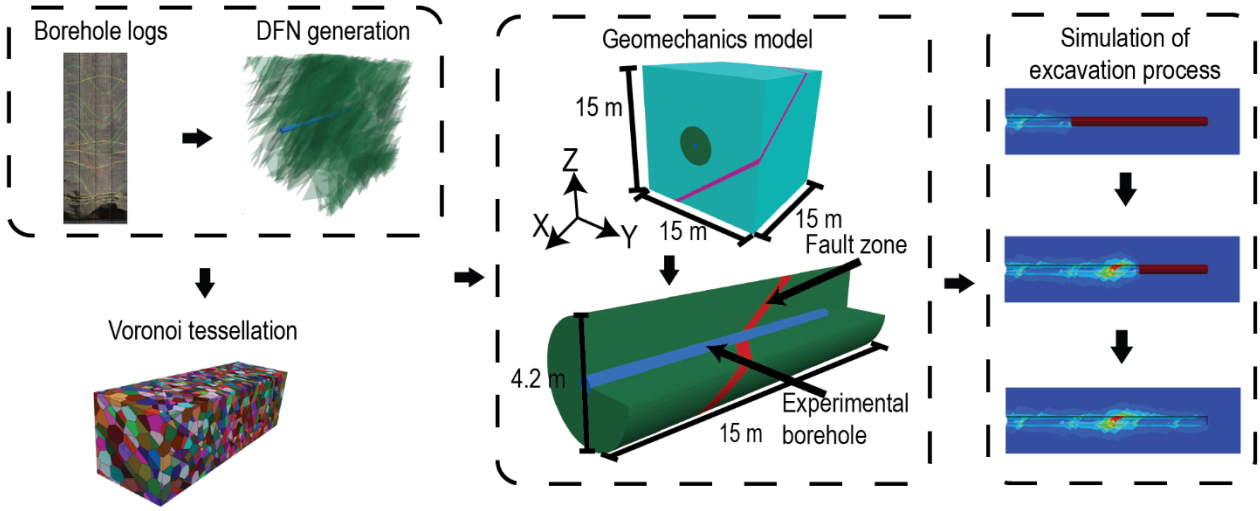

Figure 1. Workflow of 3DEC simulation of borehole excavation in faulted Opalinus Clay shale.

We assigned orthotropic elastic material properties for the Voronoi cells (i.e., intact, non-yielding rock elements) due to the presence of dominant bedding planes. Excavation-induced new crack growth is mimicked as the breakage of virtual joint elements in between Voronoi cells (Figure 2a) governed by the bi-linear Mohr-Coulomb law with softening (Figure 2b). Material properties are shown in Table 1. Initially higher strength properties (e.g., cohesion, friction angle, tensile strength, etc.) are assigned to the virtual joint elements to reflect the stronger bonding of intact rocks. However, once virtual joint elements are damaged, they evolve into broken joint elements with reduced strength properties. The mechanical behavior of fractures follows the bi-linear Mohr-Coulomb law constrained by available triaxial testing results of Opalinus Clay samples (Thoeny 2014; Wild & Amann 2018a, 2018b). The stress boundary condition of our model is informed by an existing large-scale FLAC 3D model that provides a realistic calculation of the local stress field around Niche MI, where the experiment was conducted (D. Jaeggi, pers. comm.).

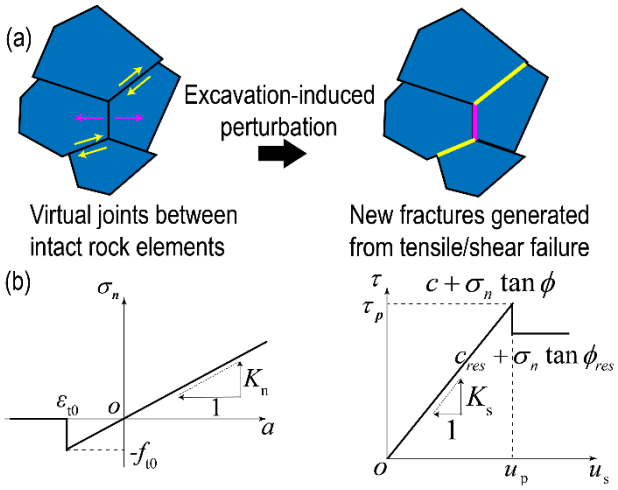

Figure 2. (a) Formation of new fractures mimicked as the breakage of virtual joints between Voronoi cells governed by (b) the bi-linear Mohr-Coulomb law with softening.

We run the short-term numerical simulation in two steps. Firstly, the model is solved under the given boundary and gravitational stress field to reach an equilibrium state. Secondly, we simulate the excavation process of the experiment borehole by sequentially removing the rock material inside the borehole in steps (with a 1-m interval), during which we capture essential excavation-induced geomechanical responses including rock mass deformation, shear slip of existing faults, and new crack growth, which we compare with the short-term behavior recorded by a borehole photogrammetric survey (e.g.,

borehole breakout locations, fracture offsets). Later work will address the influence of saturation variation and creep behavior after the excavation, to investigate the long-term progressive damage evolution.

Table 1. Material properties used in the model based on

Material properties	Value
Intact rock mass for inner region:	
Density (ρ)	2450 kg/m^3
Young's modulus parallel to bedding ($E_{i1} = E_{i2}$)	6.0 GPa
Young's modulus perp. to bedding (E_{i3})	2.0 GPa
Shear modulus parallel to bedding (G_{i12})	2.5 GPa
Shear modulus perp. to bedding ($G_{i13} = G_{i23}$)	1.15 GPa
Poisson's ratio (ν_i)	0.2
Cohesion below threshold (c_{r1})	0.6 – 1.5 MPa
Cohesion above threshold (c_{r2})	1.5 – 4.0 MPa
Friction angle below threshold (ϕ_{r1})	30 – 43°
Friction angle above threshold (ϕ_{r2})	11°
Tensile strength (σ_{ri})	0.6 – 1.2 MPa
Fractured rock mass for outer region:	
Density (ρ)	2450 kg/m^3
Young's modulus parallel to bedding ($E_{f1} = E_{f2}$)	6.0 GPa
Young's modulus perp. to bedding (E_{f3})	0.8 GPa
Shear modulus parallel to bedding (G_{f12})	2.5 GPa
Shear modulus perp. to bedding ($G_{f13} = G_{f23}$)	0.5 GPa
Poisson's ratio (ν_f)	0.2
Fault zone:	
Density	2450 kg/m^3
Young's modulus (E_{fz})	0.8 GPa
Poisson's ratio (ν_{fz})	0.3
Fracture:	
Cohesion below threshold (c_{f1})	0.2 MPa
Cohesion above threshold (c_{f2})	0.6 MPa
Friction angle below threshold (ϕ_{f1})	22°
Friction angle above threshold (ϕ_{f2})	11°
Tensile strength (σ_{ft})	0.6 MPa
Normal stiffness (k_{fn})	10 GPa/m
Shear stiffness (k_{fs})	1 GPa/m

4. Preliminary results

Some preliminary simulation results are shown in Figure 3. A conspicuous structurally-controlled pattern can be seen in the displacement field (Figure 3a). An intensively perturbed zone is located near the intersection between the borehole and the major fault zone, while some strain concentrations are also observed near the location of pre-existing fractures. The extent of the displacement field at these locations is 1–2 times the size of the borehole diameter. The largest radial extent of stress perturbation is located near the MI niche surface and also around the fault zone, and the perturbation seems to reduce with the borehole depth (Figure 3b). In the near-field of the borehole, more intense stress concentrations take place around 4–6 and 10–12 o'clock around the borehole looking West (along the negative x direction), which agrees well with the zones of in-situ borehole breakout locations as observed in the experiment. Cross sectional views at 5–10 m distances from the borehole mouth of Figure 3c illustrate the anisotropic and fracture-controlled stress concentration. At places, the discrete fracture network limits the extent of stress perturbations. However, the fault zone seems to promote higher stress levels considerably far away (1–3 experiment borehole diameters) from the experiment borehole. Stress concentrations caused a localized growth of new fractures in the near-field of the borehole and more scattered damage evolution at greater depths (Figure 3d).

To sum up, a 3-D discrete element model has been built to simulate the perturbation induced by borehole excavation in Opalinus Clay shale. The disturbance in the stress/displacement field and new crack growth have been simulated and show the evolution a clearly structurally-controlled pattern. In the future, we will further compare the simulated overbreak pattern with the in-situ observation data to gain more quantitative insights into the underlying physical mechanisms that

drive the overbreak phenomenon. We will also further develop the model to simulate the long-term failure evolution around the borehole considering rock creep behavior and saturation variation during the ventilation phase.

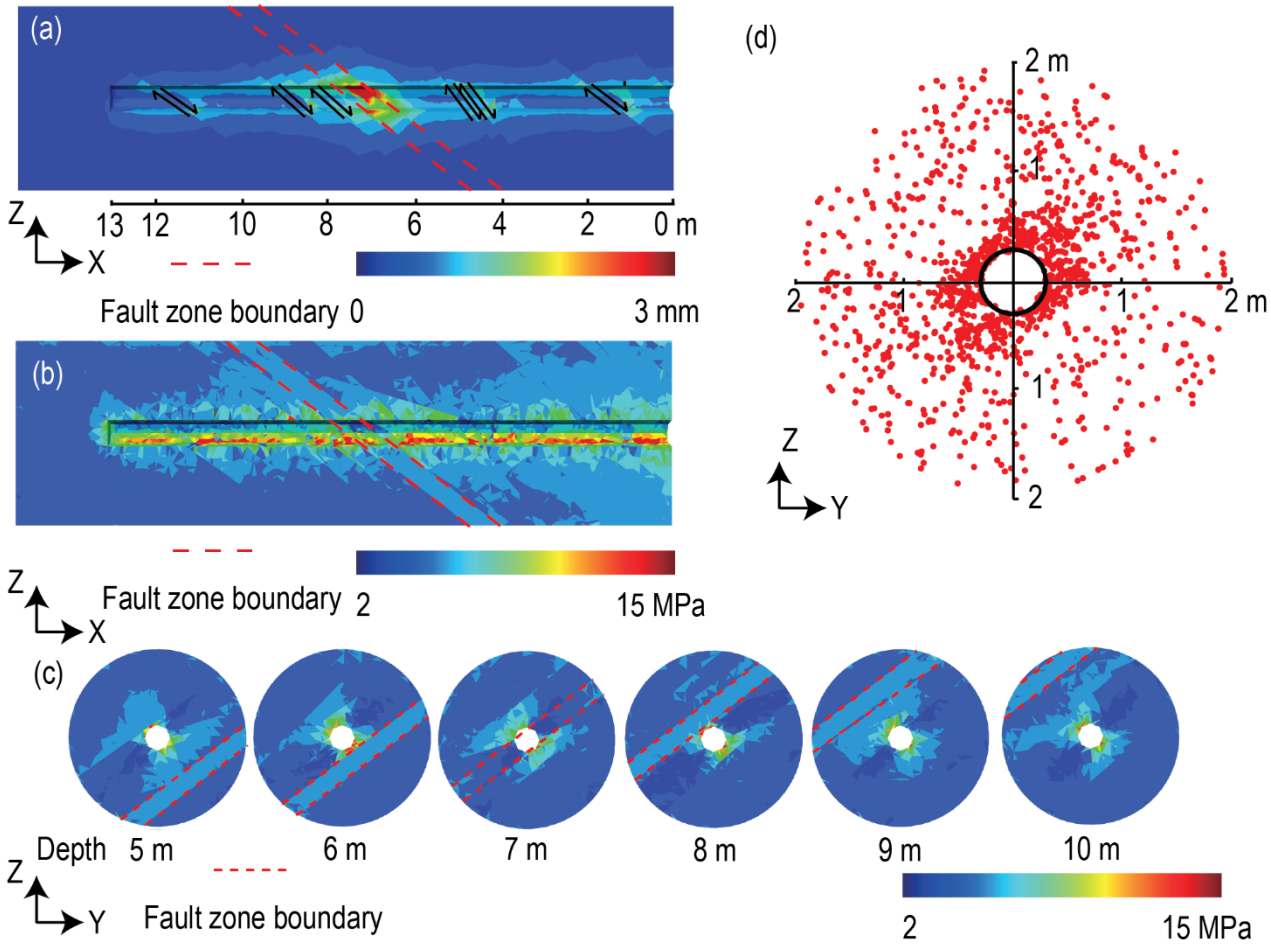

Figure 3. Preliminary results of short-term 3DEC simulation: (a) displacement field and (b) von Mises stress after excavation; (c) von Mises stress at different depths, and (d) distribution of damaged virtual joint elements along the experiment borehole axis.

5. Acknowledgement

The Swiss Federal Nuclear Safety Inspectorate (ENSI) and the Swiss Federal Office of Topography (swisstopo) are funding the PF experiment led by the Chair of Engineering Geology at ETH Zurich. We are also grateful to our partners from the Swiss Seismological Service (SED) and the German Federal Institute for Geosciences and Natural Resources (BGR).

6. Reference list

Martin, C. D. & Christiansson, R. (2009). Estimating the potential for spalling around a deep nuclear waste repository in crystalline rock. *International Journal of Rock Mechanics and Mining Sciences*, *46*(2), 219–228. https://doi.org/10.1016/j.ijrmms.2008.03.001

Martin, C. D. Kaiser, P. K., & Christiansson, R. (2003). Stress, instability and design of underground excavations. *International Journal of Rock Mechanics and Mining Sciences*, *40*(7–8), 1027–1047. https://doi.org/10.1016/S1365-1609(03)00110-2

Martino, J. B. & Chandler, N. A. (2004). Excavation-induced damage studies at the Underground Research Laboratory. *International Journal of Rock Mechanics and Mining Sciences*, *41*(8 SPEC.ISS.), 1413–1426. https://doi.org/10.1016/j.ijrmms.2004.09.010

Read, R. S. (2004). 20 years of excavation response studies at AECL's Underground Research Laboratory. *International Journal of Rock Mechanics and Mining Sciences*, *41*(8 SPEC.ISS.), 1251–1275. https://doi.org/10.1016/j.ijrmms.2004.09.012

Thoeny, R. (2014). *Geomechanical Analysis of Excavation-Induced Rock Mass Behavior of Faulted Opalinus Clay At the Mont Terri Underground Rock Laboratory* (Issue 21415). ETH Zurich.

Wild, K. M. & Amann, F. (2018a). Experimental study of the hydro-mechanical response of Opalinus Clay – Part 1: Pore pressure response and effective geomechanical properties under consideration of confinement and anisotropy. *Engineering Geology*, *237*(April 2017), 32–41. https://doi.org/10.1016/j.enggeo.2018.02.012

Wild, K. M. & Amann, F. (2018b). Experimental study of the hydro-mechanical response of Opalinus Clay – Part 2: Influence of the stress path on the pore pressure response. *Engineering Geology*, *237*(April 2017), 92–101. https://doi.org/10.1016/j.enggeo.2018.02.011

Ziegler, M. & Loew, S. (2020). Mont Terri PF experiment: Progressive failure of structurally-controlled overbreaks — Project introduction and overview of work program. ENSI Research and Experience Report 2019, ENSI-AN-10919, 307–315.